FLUORESCENCE POLARIZATION SPECTROSCOPY AND TIME-RESOLVED FLUORESCENCE KINETICS OF NATIVE CANCEROUS AND NORMAL RAT KIDNEY TISSUES

Darayash B. Tata, Marina Foresti, Julius Cordero, Philip Tomashefsky,*
Michele A. Alfano, and R. R. Alfano
*Institute for Ultrafast Spectroscopy and Lasers, Department of Physics, The City College of New York,
New York, New York 10031; and *College of Physicians and Surgeons, Urology Department, Columbia
University, New York, New York 10032*

ABSTRACT Steady state fluorescence polarization spectra and time-resolved emission decay kinetics have been measured in vitro from malignant and normal rat kidney tissue. The degrees of polarization and emission lifetimes from the cancerous and normal systems are different. The spectroscopic differences are attributed to environmental transformations local to the native flavin and porphyrin fluorophors' binding sites.

INTRODUCTION

Absorption and emission polarization spectroscopy have served as useful tools for identifying fluorophor electronic states and conformational structures in different environments. It has been well established that the polarized spectroscopic properties of the fluorophors are highly dependent on polarity, pH, and viscosity. Depolarization studies of known fluorophors are currently utilized as probes to investigate their local environment. A definite correlation exists between the loss in the degree of polarization and environmental influences (1, 2). Extrinsic fluorescent dye molecules with known emission properties have been conjugated to nonemitting protein molecules in order to perform polarization studies that help elucidate protein structure, molecular dynamics, and characteristics of the local environment (3). There are known native protein-bound fluorophors within cells such as flavins and porphyrins that fluoresce in the visible. Recently, we reported on the differences between native visible fluorescence spectra from normal and cancerous rat tissues (4). The measured changes in the spectral features between the cancerous and normal tissues were attributed to environmental transformation and/or to charge buildup in the cancerous cells.

In this communication, the visible polarization fluorescence spectra and fluorescence lifetimes of cancerous and normal rat kidney tissues have been measured. We show that there are spectroscopic differences between the two tissues. Qualitative information on the local environment surrounding the native flurophors (flavins and porphyrins) at their binding site within normal and cancerous tissue was obtained from the fluorescence depolarization and lifetime data.

MATERIALS AND METHODS

Fluorescence Polarization Spectra Method

A schematic diagram of the experimental apparatus used to measure the steady state degree of fluorescence polarization from the rat kidney normal and malignant tissues is shown in Fig. 1 A. A 100-mW argon ion laser operated at 488 nm was linearly polarized in a fixed vertical direction, and was then focused on the front surface of the tissue to a spot size of ~100 μm. The laser was chopped at 200 Hz. The luminescence from the front surface was collected and passed through an analyzer, which had its optical axis set parallel or perpendicular to the incident linearly polarized lasar light. The parallel or perpendicular polarized luminescence was passed through a depolarizer at the front entrance slit of a double ½ m grating scanning spectrometer (Spex Industries, Inc., Edison, NJ) blazed at 500 nm. The presence of the depolarizer ensured that the spectrometer had not given any preference to any one of the two selected directions of the polarized luminescence. A photomultiplier tube (PMT) [Model 7265 (S-20); RCA, Lancaster, PA], located at the exit slit of the spectrometer measured the intensity at different wavelengths. The spectral resolution was 1.8 nm. The output of the PMT was connected to a lock-in amplifier (EG & G Princeton Applied Research, Princeton, NJ) and an X-Y recorder combination to display each spectrum. The intensity of the parallel or perpendicular components of the sample's luminescence as functions of wavelengths were each measured on separate scans. The degree of polarization was computed from the equation: $P(\lambda) \sim [I_{\parallel}(\lambda) - I_{\perp}(\lambda)]/[I_{\parallel}(\lambda) + I_{\perp}(\lambda)]$. The $I_{\parallel}$ and $I_{\perp}$ spectra were not corrected for the spectral response of the system. Each tissue samples $I_{\parallel}$ and $I_{\perp}$ were recorded and the degree of polarization computed three separate times to check reproducibility.

Fluorescence Kinetics Method

Picosecond fluorescence time-resolved measurements from both rat kidney normal and tumor tissues were performed using a streak–camera mode locked laser system (Fig. 1 B). A single 8-ps, 353-nm pulse was used to excite the sample, using a third harmonic of an Nd–glass laser. The sample was excited on the front surface of the tissue and the fluorescence focused on a 50-μm slit of a streak camera (Hamamatsu Corp., Middle-
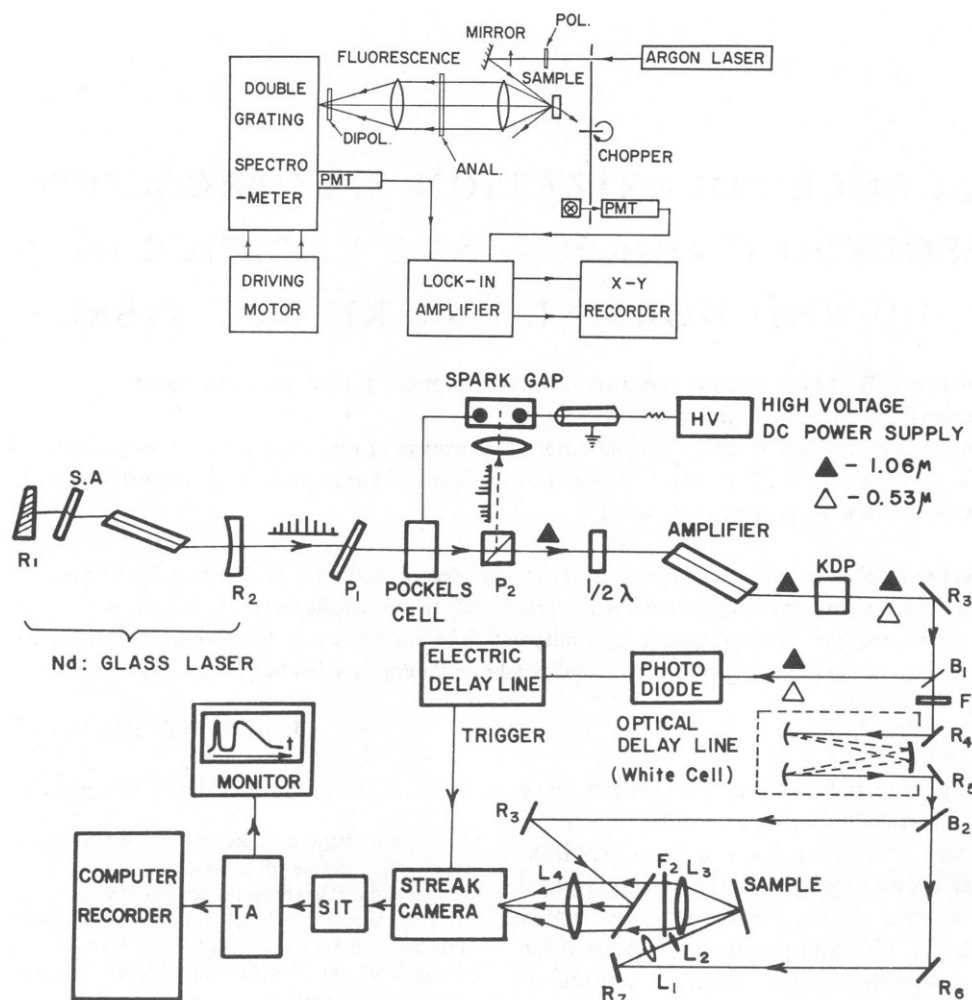
FIGURE 1 (*A*) Schematic diagram of the steady state fluorescence degree of polarization apparatus. (*B*) Schematic diagram of the time-resolved fluorescence experimental setup.

sex, NJ). All measurements were performed at room temperature. The excitation pump pulse was at 353 nm, and was separated from the 1,059-nm and 527-nm pulses with 7-51 and 7-60 filters (Corning Glass Works, Corning, NY). Filters were used to select the desired wavelength bands to be analyzed. The fluorescence kinetics analyzed in the band region of 500–550 nm had been selected using a shortpass 560 filter, coupled to 3-70 and 3-71 filters (Corning Glass Works). The fluorescence kinetics analyzed in the band regions of 550–600 nm had been investigated using a shortpass 660-nm and 3-67 (Corning Glass Works) filters.

The streak camera was coupled to a video camera. The data were acquired by a temporal analyzer (Hamamatsu Corp.) and processed in a DEC-11 Minc mini-computer (Digital Equipment Corp., Marlboro, MA), for collection and final analysis. The fluorescence curves were corrected for time and intensity nonlinearities. The fitting of the final curves was performed using the least-squares method.

Sample Preparation Method

The polarization and time-resolved lifetime data were obtained from in vitro cancerous and normal rat kidney tissues. The kidney tumor was subcutaneously implanted in Wistar/Lewis rats. The rats were 4 wk old at the time of testing. All tissue samples were nonnecrotic and weighed ~1 g. All tissue samples were solid chunks, not cut to any particular specificity, and were a few millimeters thick. Each tissue sample was placed in a clean optical flurometric cuvette (Markson Science Inc.,

Phoenix, AZ) for these spectroscopic studies. Samples were run within 2 h after removal on the same day of extraction. Measurements were made at least four times each on all four samples to assure reproducibility. Four different samples were tested from different rats.

RESULTS

Steady State Fluorescence Polarization Spectra

The polarized-fluorescence spectra from normal and tumor rat kidney tissues excited at 488 nm are shown in Figs. 2 *A* and *B*, respectively. In each of these figures, a pair of relative fluorescence intensity components $I_{\parallel}$ and $I_{\perp}$ from their respective tissues are displayed. The spectral profiles of rat kidney tumor tissues are seen to be substantially different from their normal counterparts. These spectra are consistent with our previously reported observations (4).

The principal maxima of the spectra from rat kidney normal and tumor tissues are located at 531 and 521 nm, respectively. For the normal rat kidney tissues, the width of
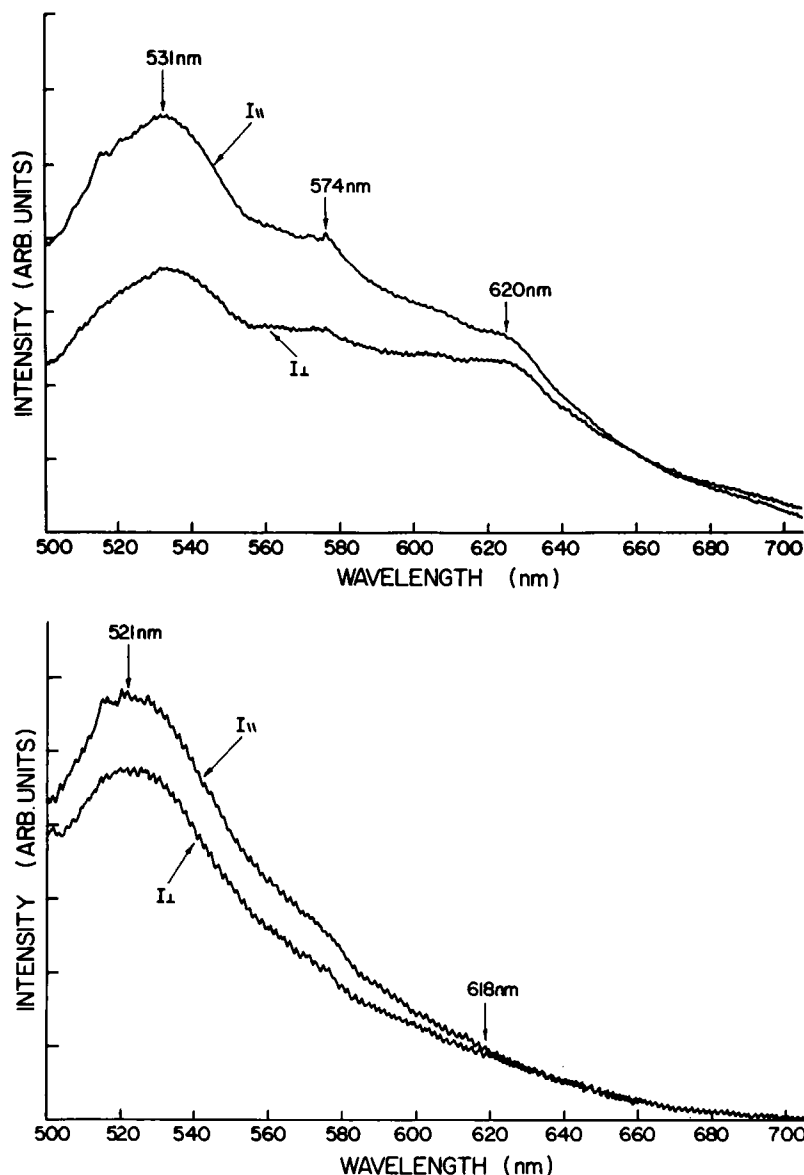
FIGURE 2 (A) Parallel and perpendicular fluorescence intensity components emitted from rat normal kidney tissue. (B) Parallel and perpendicular fluorescence intensity components emitted from rat kidney tumor tissue.

the principal maxima of the two polarized intensity components are seen to be virtually the same, spanning ~38 nm. On the ascending side of the principal maxima, one observes the differences in the spectral profiles between the parallel and perpendicular intensity components. The $I_\perp$ spectral profile increases monotonically toward its apex, whereas the $I_\parallel$ component spectral profile exhibits a gradual increase toward its peak, superimposed by additional spectral features of a small secondary peak and a shoulder. At the prominent peak, the parallel component is seen to fluoresce ~1½ times more intensely than $I_\perp$ component. After the prominent maxima, both intensity component spectra, $I_\parallel$ and $I_\perp$ from the rat kidney normal tissues are seen to decrease monotonically. There are two subsidiary maxima located at 574 and 620 nm.

The general spectral profiles along this declining side of

the curves are closely similar to each other, even though the monotonic rate of decline is faster for the $I_\parallel$ spectrum. At 656 nm the spectral curves coincide, after which the $I_\perp$ component spectrum continues to decline toward zero at a faster rate than the $I_\perp$ spectrum.

The tumor's principal maximum is recorded as 10 nm blueshifted with respect to the normal tissue's principal maximum. The spectra possess a smaller half-width peak spanning ~15 nm. At the principal maxima, one observes that $I_\parallel$ and $I_\perp$ have nearly the same magnitude. After the prominent maxima, both $I_\parallel$ and $I_\perp$ decline monotonically and there are no additional subsidiary maxima recorded. Specifically, the secondary peak located 620 nm in the normal tissue's component spectrum is not observed in the tumor sample. The intensity components' spectral profiles are similar to each other, even though the monotonic rate

of decline is faster for the $I_{\perp}$ spectrum. At 618 nm both curves coincide and thereafter monotonically fall toward zero intensity.

Fig. 3 displays the computed polarized emission spectra of rat kidney tumor and normal tissues. The salient features of the two spectral profiles is the low degree of polarization exhibited by the tumor tissues, and the large and smoothly varying degree of polarization from the normal tissues. The normal kidney polarized spectrum peaks at 520 nm, ~25% degree of polarization, and smoothly declines up to 570 nm, after which it undergoes a rapid loss in polarization, declining monotonically to zero at 650 nm. The tumor polarized spectrum profile is seen to oscillate about a 10% polarization value up until 585 nm, after which it sharply drops to a lower average oscillation value of 6.5% for the next 30 nm. The polarization signal sharply drops to zero after 618 nm.

Fluorescence Kinetics

Typical lifetime decay kinetic profiles for normal and tumor tissues investigated in the 500–550-nm and 550–650-nm wavelength bands are shown in Figs. 4 and 5, respectively.

The kinetic curves are interpreted as a combination of a rapidly decaying component and a slowly decaying component. The experimental data are fitted to a double exponential curve given by $I(t) = A_F e^{-t/t_f} + A_S e^{-t/t_s}$ for all the sets of data collected. The data for different emission bands for each tissue are summarized in Table I. The table shows the lifetime measured for the fast and slow component, both of normal and tumor tissues in emission band of the flavins (500–550 nm), and in the emission band of the porphyrins (600–650 nm). The amplitude values shown in

the table are proportional to the intensity and normalized for the gain and filter transmission.

For the 500–550-nm spectral region, the fluorescence decay lifetimes of the fast and slow components from the normal tissue's flavin emission band were 357 ±18 ps and 1,220 ±35 ps, respectively. The time for the intensity maxima of normal tissue to drop to $1/e$ its value was ~900 ps. For the tumor tissue, the fast component decay time was 223 ±15 ps, and that of the slow component was 1,966 ±37 ps. The ratios of fast to slow amplitude values for normal and tumor tissues were 0.6 and 1.43, respectively. The time for the intensity maxima to drop to $1/e$ value was faster for tumor tissue, ~450 ps.

For the 550–650 nm spectral region, the normal tissue sample decay lifetimes measured were 204 ±11 ps and 1,000 ±6 ps, for the fast and slow components, respectively. For the tumor tissue, the fast component decay time was 236 ± 14 ps, and the slow component one was 1,963 ± 37 ps. The ratios of fast to slow amplitude values for normal and tumor tissues were 0.86 and 2, respectively. The time for the intensity maxima to drop to $1/e$ values for the normal and tumor tissues was about the same, 350 ps.

The time-resolved measurements display an outstanding feature in the slow component lifetime values of the two contrasting tissues. The tumor tissue's slow component lifetime measurements have yielded very nearly similar values around 2 ns, in the two spectral regions investigated. Normal tissue's slow component lifetimes, in the two spectral regions analyzed, were also almost similar (~1 ns). The tumor tissue's slow component lifetimes, for both spectral regions, were longer by a factor of two, compared with the slow component of its normal counterpart.

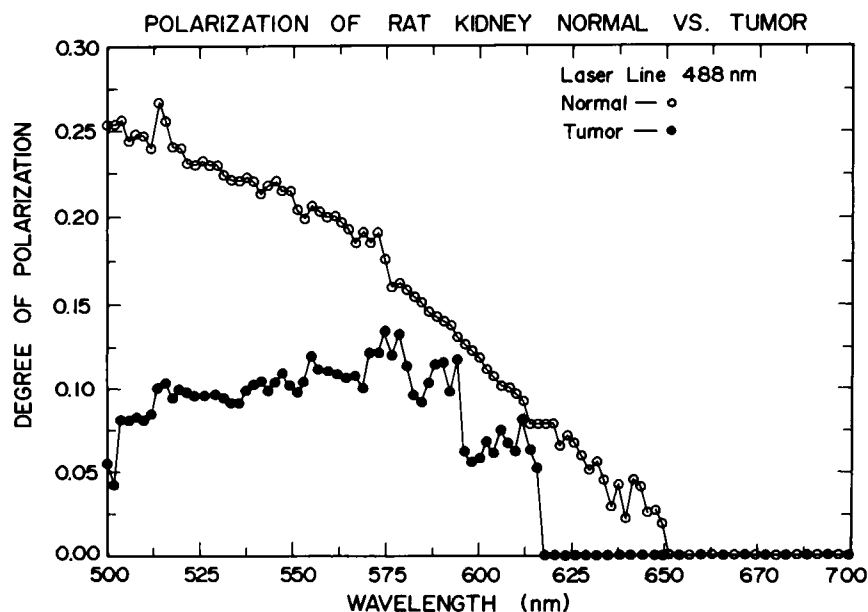Another significant difference occurred in the fast com-

FIGURE 3 Degree of fluorescence polarization spectra from rat kidney normal and tumor tissues.
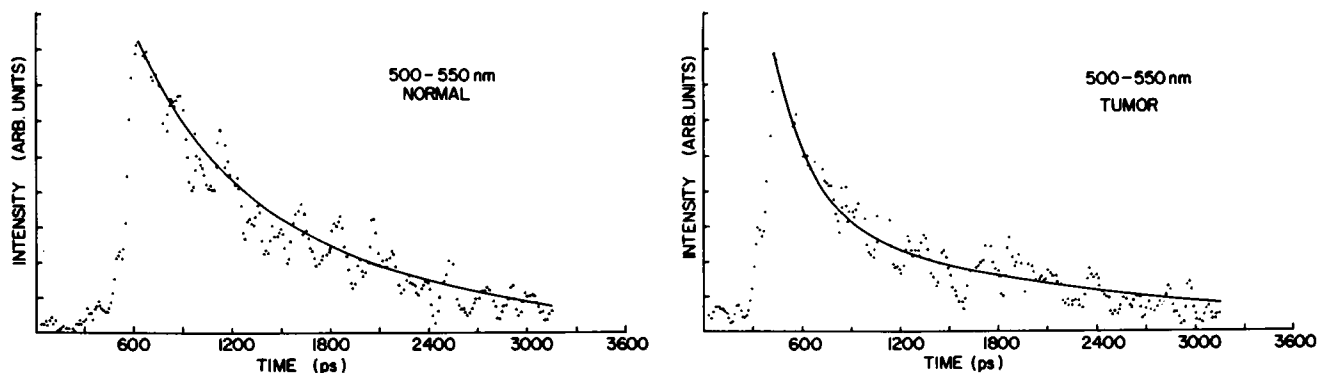
FIGURE 4 (*A*) Normal tissue's fluorescence kinetics measured within 500–560-nm spectral region. $t_F - 350$ ps. $t_s - 1,200$ ps. $A_F - 47, A_S - 158$. (*B*) Tumor tissue's fluorescence kinetics measured within 500–560-nm spectral region. $t_F - 235$ ps. $t_s - 1,950$ ps. $A_F - 117. A_s - 78$.

ponent lifetimes of the normal and malignant tissues observed within the flavins emission region (500–560 nm). The fast component lifetimes are 360 ps for the normal tissue and 220 ps for the malignant tissue. In the 550–650-nm spectral region, the fast component lifetimes of the two contrasting tissues were approximately of the same order of 220 ps. Furthermore, the ratios of slow to fast amplitude were consistent for both hands.

DISCUSSION

Fluorescence Polarization Spectra

The fluorescence spectra of the native fluorophors within the intact cells display unique sets of spectral features that most likely characterize their local environment and the state of the cells making up the kidney tissues. The observed 10-nm blueshifts in the prominent peaks and the disappearance of secondary spectral peaks at longer wavelengths, discovered in the kidney tumor fluorescence spectra, may be attributed to the kidney cells' physiological and biochemical transformations from the norm. Previous fluorescence studies have shown that when protein-containing fluorophors gain positive charge ions, their fluorescence spectral maxima have been noted to be blueshifted (5). Past research with intact Ehrlich ascites tumor cells sug-

gests that tumor cells take up and entrap cations such as Ca^{+2}, K^+, and Mg^{+2} to a greater degree than their normal counterparts (6). Hence, our observed 100-nm blueshift in the prominent maxima of the kidney tumor suggests an accumulation of positively charged ions in the malignant cells' intracellular environment. The majority of the coenzyme flavins and flavoproteins are known to fluoresce about 520–530 nm due to their S_1 to S_0 transitions (7, 8). Our measured broad fluorescence maximum at 530 nm for the normal kidney tissue is attributed to the superposition of fluorescence peaks from many species of flavin-bound proteins and enzymes. The contracted spectral width of the prominent maximum in the tumor's emission spectra about the 520-nm region may indicate that some of the flavin species are quenched or are absent.

The emission spectra of normal tissues show evidence of other fluorescing species which contribute to secondary spectral peaks. The secondary peak about the 600-nm region may be attributed to porphyrins. Depending on the environment, the principal bands of the various porphyrins lie between 597 and 634 nm (1). In an acidic environment, coroporphyrin and protoporphyrin have their bands at 597 and 630 nm, respectively (1, 9). In organic solvents their respective principal bands are at 625 and 634 nm. One may conjecture that the secondary spectral peaks observed from
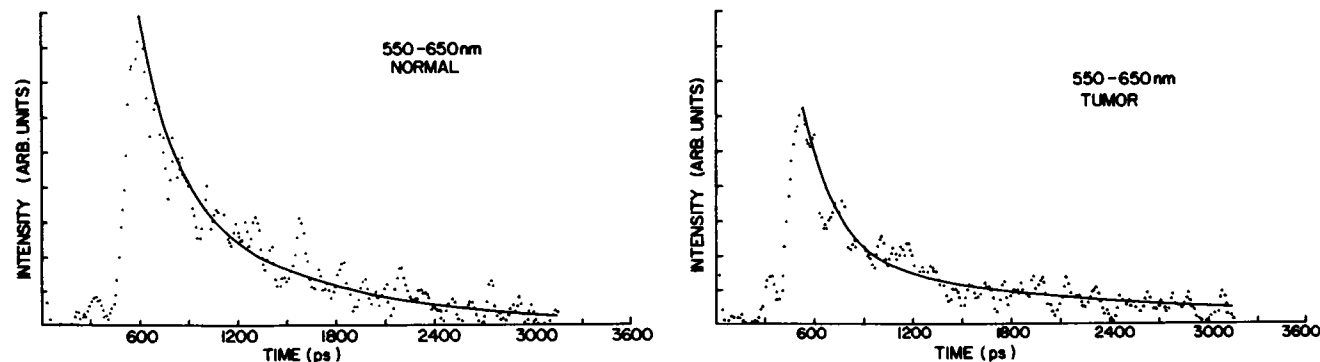

FIGURE 5 (*A*) Normal tissue's fluorescence kinetics measured within 550–650-nm spectral region. $t_F - 200$ ps. $t_s - 900$ ps. $A_F - 115. A_s - 106$. (*B*) Tumor tissue's fluorescence kinetics measured within 550–650-nm spectral region. $t_F - 220$ ps. $t_s - 1,450$ ps. $A_F - 112. A_s - 43$.

Tissues	Region analyzed	t_f	t_s	A_f/A_s	$T_{1/e}$
	nm	ps ± SD	ps ± SD		ps
Normal	500–550	357 ± 18	1,220 ± 35	0.6	900
Tumor	500–550	223 ± 15	1,966 ± 37	1.43	450
Normal	550–650	204 ± 11	1,000 ± 63	0.86	390
Tumor	550–650	236 ± 14	1,963 ± 37	2.0	350

normal rat kidney tissues may have arisen from enzymatically reduced heme proteins. The normal kidney tissues were seen to be engorged with blood, giving them a red appearance; however, the rat kidney tumor tissues were observed to be white, nearly devoid of blood, a consequence of rapid growth of the tumor. As a result of this decrease in blood flow per weight of tissue one would expect a substantially smaller amount of reduced heme porphyrins which could contribute to the tumor tissue's fluorescence around the 600-nm region.

The degree of polarization from the native fluorophors of the rat kidney normal and tumor tissues exhibits unique spectral features that may characterize the pathological state of the cells making up the tissues. Both rotational motions and energy-transferring mechanisms are expected to have participated in depolarizing the emission from the native fluorophors. Previous polarization studies on fluorophors in low to moderate viscosities at room temperature have revealed the Brownian rotational depolarizing mechanism to be dominant over other energy transferring depolarizing mechanisms. The normal tissue's degree of polarization at the 530-nm fluorescence component maxima is noted to be 22%, whereas the emission polarization value from the tumor tissue's prominent maxima at 520 nm is seen to be ~10%. The difference suggests that either most of the flavins are in closer proximity to each other in the cancerous tissues than in the normal tissues, so that depolarization through energy migration becomes more effective, or that the flavins within the malignant cells have greater freedom of rotational mobility. The latter case is more likely.

As a first order approximation, one can calculate the rotational diffusion times of the flavins within the two contrasting cellular environments, through the use of Perrin's Equation (10): $(1/P - 1/3) = (1/P_0 - 1/3)(1 + T_F/T_{rot})$ where P is the experimentally measured steady state degree of polarization, P_0 is the maximum polarization of the fluorophors when depolarizing effects are absent, T_F is the excited state relaxation lifetime, and T_{rot} is the rotational diffusion time. The flavins' rotational motions are considered to be isotropic and similar species of flavins are assumed to be involved in giving identical maximum polarization value P_0 from the normal and cancerous

systems. Polarization studies of several flavin-bound coenzymes in highly viscous media at subzero temperatures have yielded similar maximum degree-of-polarization values, ~43% (10). The average fluorescence $1/e$ relaxation lifetimes measurements of the S_1 to S_0 flavin transitions from the normal and cancerous systems have yielded $T_{F\,normal} = 900$ ps, and $T_{F\,cancer} = 450$ ps. The rotational diffusion times of the flavins within the environment of the two systems are computed from the Perrin Equation. This yields $T_{rot\,norm} = 808$ ps and $T_{rot\,cancer} = 117$ ps. Thus, the low degree of polarization from the flavin fluorophors of the cancerous cells is most probably attributed to their fast $T_{rot\,cancer}$ as compared to $T_{rot\,norm}$. This indicates that the flavin fluorophors are more loosely bound to the enzymes and proteins within the intracellular environment of the cancerous cells.

It is intriguing to observe that the fluorescence polarization features from the normal tissues strongly resemble the riboflavin emission polarization spectrum, up to 570 nm (see, for example, Ref. 11). The polarization maximum at 515 nm is coincident with the riboflavins' polarization maximum. The smooth monotonic depolarization of the native flavins' emission from the normal kidney tissues may signify the presence of other native species of fluorophors which have their absorption band overlapping the flavins' emission band. The porphyrins are chemical species that are known to satisfy this spectroscopic requirement (9). The normal tissue's leveled polarization signal between 615 and 625 nm has most probably arisen from reduced hemeporphyrins. The emission polarization signal arising from the native flavins of the cancerous tissues was seen to be level and gives no spectroscopic evidence for the presence of secondary depolarizing species.

Fluorescence Kinetics

The following model, consistent with the steady state polarization data, is used to help explain the observed recombination decay times for the flavins' (500–550 nm) main emission band for the normal and tumor tissues. The fast and slow decay components may be due to the type of local interactions of the environment with the flavin species. The fast decay component is likely to be associated with highly mobile species of flavin fluorophors that are constrained by their local cellular environment. The slow component, on the other hand, may be associated with the coupling and energy transfer routes of the flavin fluorophors to the surrounding protein media. The slower component relaxation time of the flavins within the cancerous system was nearly twice the lifetime of the flavins within normal systems. This result indicates that there is a smaller number of nonradiative pathways by which energy can be transferred away from the protein linked flavins within the malignant environment, than within the normal environment. The flavin fluorophors in the cancerous media

weaken their linkage and interactions with the enzymes and proteins. The fluorophors in effect become freer. In this state the fast component should be expected to become faster than in its normal counterpart because of the additional dynamic quenching pathways created by the increased rotational and translational freedom. The overall $1/e$ times in both types of tissues are in agreement with this model. This interpretation is also consistent with the twofold lower degree of polarization from the flavin band measured in the cancer tissues compared with the normal tissues. A similar trend is observed in 600–650 nm slow component band; however, the fast-component recombination and $1/e$ times are not altered. The twofold larger ratio of fast to slow amplitudes for tumor tissue compared with normal tissue indicates that there are more "free" flavin fluorophors within the malignant environments than in their normal environment. This is also consistent with the above model.

REFERENCES

1. Udenfriend, S. 1969. Fluorescence Assay in Biology and Medicine. Vol. 1 and 2. Academic Press Inc., New York.

2. Campbell, I. D., and R. A. Dewk. 1984. Biological Spectroscopy. Benjamin/Cummings Publishing Company Inc., Reading, MA. 98–115.

3. Stryer, L. 1968. Fluorescence spectroscopy of proteins. *Science (Wash. DC).* 162:526–533.

4. Alfano, R. R., D. B. Tata, J. J. Cordero, P. Tomashefsky, F. W. Longo, and M. A. Alfano. 1984. Laser induced fluorescence spectroscopy from native cancerous and normal tissues. *IEEE J. Quantum Electron.* 20:1507–1511.

5. Honig, B. 1982. Theoretical aspects of photoisomerization. *In* Biological Events Probed by Ultrafast Laser Spectroscopy. R. R. Alfano, editor. Academic Press Inc., New York. 285.

6. Wenner, C. E. 1975. Cancer. Vol 3. Biology of Tumors: Cellular Biology and Growth. F. F. Becker, editor. Plenum Publishing Corp., New York. 394–398.

7. Chance B., and B. Schoener. 1966. Fluorometric studies of flavin compounds of the respiratory chain. *In* Flavins and Flavoprotein. E. C. Slater, editor. Elsevier North-Holland Scientific Publishers, Ltd., Amsterdam, The Netherlands.

8. G. D. Fasman, editor. 1975. Handbook of Biochemistry and Molecular Biology. 3rd ed. CRC Press, Inc., Cleveland, OH. 205–210.

9. Adar, F. 1978. The Porphyrins. Vol. 3. D. Dolphin, editor. Academic Press, Inc., New York. 167–182.

10. Weber, G. 1966. Fluorescence and Phosphorescence Analysis. Chapter 8. D. M. Hercules, editor. John Wiley & Sons, New York.

11. Kurtin, W. E., and P.-S. Song. 1968. Photochemistry of the model phototropic system involving flavins and indoles. I. Fluorescence polarization and moment calculations of the direction of the electronic transition moment in flavins. *Photochem. Photobiol.* 7:263–273.